ACS Medicinal Chemistry Letters

Letter

pubs.acs.org/acsmedchemlett

Design and Synthesis of $mGlu_2$ NAMs with Improved Potency and CNS Penetration Based on a Truncated Picolinamide Core

Katrina A. Bollinger,[‖] Andrew S. Felts,[†,‖] Christopher J. Brassard,[†,‖] Julie L. Engers,[†,‖] Alice L. Rodriguez,[†,‖] Rebecca L. Weiner,[‖] Hyekyung P. Cho,[†,‖] Sichen Chang,[‖] Michael Bubser,[†,‖] Carrie K. Jones,[†,‖,§] Anna L. Blobaum,[†,‖] Colleen M. Niswender,[†,‖,§] P. Jeffrey Conn,[†,‖,§] Kyle A. Emmitte,[†,‖,‡,⊥] and Craig W. Lindsley*[,†,‖,‡]

[†]Department of Pharmacology, Vanderbilt University School of Medicine, Nashville, Tennessee 37232, United States

[‡]Department of Chemistry, Vanderbilt University School of Medicine, Nashville, Tennessee 37232, United States

[‖]Vanderbilt Center for Neuroscience Drug Discovery, Vanderbilt University School of Medicine, Nashville, Tennessee 37232, United States

[§]Vanderbilt Kennedy Center, Vanderbilt University Medical Center, Nashville, Tennessee 37232, United States

Supporting Information

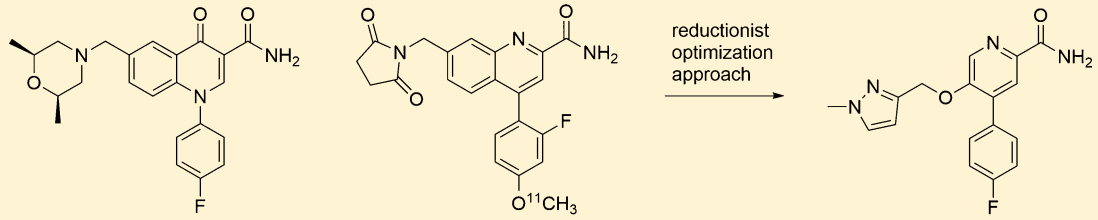

VU6001192
$mGlu_2$ IC_{50} = 207 nM
$mGlu_3$ IC_{50} > 30 μM
rat K_p = 0.2

[^{11}C]QCA
$mGlu_2$ IC_{50} = 45 nM
$mGlu_3$ IC_{50} > 30 μM
rat K_p = 0.3

VU6001966
$mGlu_2$ IC_{50} = 78 nM
$mGlu_3$ IC_{50} > 30 μM
rat K_p = 1.9

ABSTRACT: Herein, we detail the optimization of the $mGlu_2$ negative allosteric modulator (NAM), VU6001192, by a reductionist approach to afford a novel, simplified $mGlu_2$ NAM scaffold. This new chemotype not only affords potent and selective $mGlu_2$ inhibition, as exemplified by VU6001966 ($mGlu_2$ IC_{50} = 78 nM, $mGlu_3$ IC_{50} > 30 μM), but also excellent central nervous system (CNS) penetration (K_p = 1.9, $K_{p,uu}$ = 0.78), a feature devoid in all previously disclosed $mGlu_2$ NAMs (K_ps ≈ 0.3, $K_{p,uu}$s ≈ 0.1). Moreover, this series, based on overall properties, represents an exciting lead series for potential $mGlu_2$ PET tracer development.

KEYWORDS: *Negative allosteric modulator (NAM), metabotropic glutamate receptor 2 ($mGlu_2$), depression, VU6001966, CNS penetration*

The group II metabotropic glutamate receptors, $mGlu_2$ and $mGlu_3$, signal through $G_{i/o}$ to diminish cAMP production by the inhibition of adenylyl cyclase.[1−8] These presynaptic receptors are widely expressed in the mammalian central nervous system (CNS; cerebral cortex, amygdala, hippocampus, and cerebellum).[1−8] Utilizing dual $mGlu_{2/3}$ orthosteric antagonists and negative allosteric modulators (NAMs), therapeutic relevance has been established in multiple neurodegenerative (chronic pain, Alzheimer's disease (AD), Parkinson's disease (PD), drug abuse) and psychiatric (schizophrenia, anxiety, and depression) disorders.[9−14] However, the contribution due to selective $mGlu_2$ or $mGlu_3$ inhibition remains elusive; indeed, for the group II mGlu receptors, the field has only had selective $mGlu_2$ PAMs[15,16] and, only recently, selective $mGlu_3$ NAM *in vivo* tool compounds.[17−21] Furthermore, the only reported $mGlu_2$ NAMs, **1** and **2** (Figure 1), are P-gp substrates with limited CNS penetration (K_ps < 0.3), precluding their use as tools to dissect the role of selective $mGlu_2$ inhibition *in vivo* or as $mGlu_2$ PET tracers.[22,23] The development of selective and highly CNS penetrant $mGlu_2$ NAMs is clearly warranted, as $mGlu_2$, by inhibiting glutamate release, has been proposed to protect neurons from excitotoxicity in key brain regions.[24] For example, $mGlu_2$ is overexpressed in the hippocampus of Alzheimer's disease patients relative to age-matched controls.[25] In this Letter, we will detail an optimization effort based on **1** and **2** in which we undertake a reductionist approach to develop a new, minimum pharmacophore-based series of potent and selective $mGlu_2$ NAMs with exceptional CNS penetration (K_ps > 1.5)

Received: July 10, 2017
Accepted: August 2, 2017
Published: August 3, 2017

ACS Publications © 2017 American Chemical Society

DOI: 10.1021/acsmedchemlett.7b00279
ACS Med. Chem. Lett. 2017, 8, 919−924

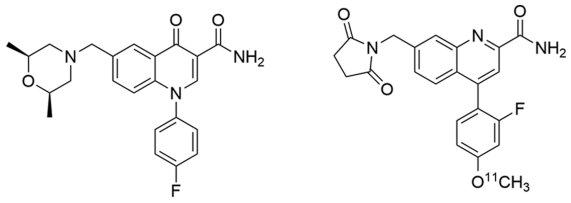

Figure 1. Structures, pharmacology, and rat CNS exposure data for $mGlu_2$ NAMs **1** and **2** reported in the primary literature.[21,22]

suitable for use as *in vivo* probes and as leads for PET tracer development.

Based on a reductionist approach to the optimization of an $mGlu_3$ NAM **3** to provide **4** (Figure 2) with improved potency

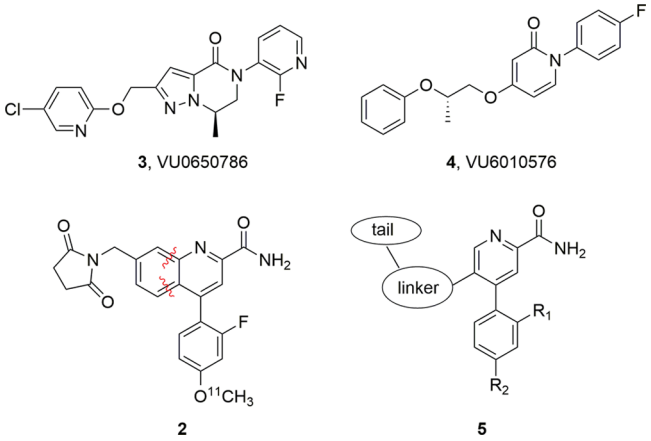

Figure 2. Structures of $mGlu_3$ NAM **3** and the optimized $mGlu_3$ NAM **4** via a reductionist approach to the minimum pharmacophore possessing the desired potency, selectivity, and CNS penetration. A similar strategy for **2** will ideally afford a simplified picolinamide-based $mGlu_2$ NAM **5** with the desired potency, selectivity, and CNS penetration.[21]

and physiochemical and DMPK properties,[21] we elected to employ a similar strategy for development of a highly CNS penetrant tool compound from $mGlu_2$ NAMs **1** and **2**. Here, we again envisioned truncating the bicyclic core of **1** and **2** to a simple picolinamide scaffold with a suitably tethered western tail moiety, represented generically by **5**.

Using **1** and **2** as leads, our goal was to reduce molecular complexity and enhance CNS penetration in a next generation $mGlu_2$ NAM suitable for *in vivo* studies and as a lead for PET tracer development to enable occupancy studies. Based on the success with $mGlu_3$ NAM **4**,[21] we truncated **2** to a simple 4-phenylpicolinamide with a pendant 5-alkoxy linker to a diverse array of aryl and heteroaryl tails. The initial structure−activity relationship (SAR) exploration evaluated the ethylenedioxy linker of **2** while holding the 4-F phenyl moiety of **1** constant. The chemistry required to access analogues **13** required eight steps (Scheme 1).[26] Starting from commercial 2,5-difluoro-4-iodopyridine **6**, a chemoselective Suzuki coupling with 4-phenylboronic acid affords **7** in 92% yield. Acidic hydrolysis affords the pyridinone **8**, which was smoothly converted to the corresponding triflate **9**. A microwave-assisted, palladium-catalyzed cyanation reaction delivers **10** in good yield. An

Scheme 1. Synthesis of Analogues 13[a]

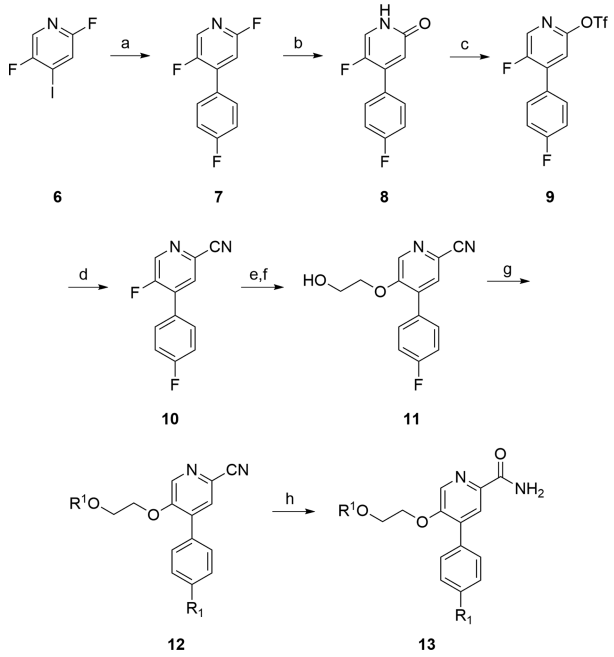

[a]Reagents and conditions: (a) 4-fluorophenylboronic acid, 10 mol % $PdCl_2$(dppf), 1 M aq. Na_2CO_3, DME, 100 °C, 92%; (b) AcOH, H_2O, 130 °C, 99%; (c) *N*-phenyl triflimide, TEA, DCM, DMF, 0 °C, 93%; (d) $Zn(CN)_2$, $Pd(PPh_3)_4$, DMF, microwave 140 °C, 15 min, 73%; (e) 2-(tetrahydro-2*H*-pyran-2-yloxy)ethanol, NaH, DMF, rt; (f) PTSA, DCM, EtOH, rt, 18 h, 65% for the two steps; (g) R^1OH, PPh_3, D^tBAD, THF, rt,18 h, 9−35%; (h) $KOSiMe_3$, THF, reflux, 85%.

S_NAr reaction with 2-(tetrahydro-2*H*-pyran-2-yloxy)ethanol and deprotection of the THP-ether provides alcohol **11**. Finally, a Mitsunobu reaction with various hydroxypyridines and nitrile hydrolysis to the primary carboxamide gives putative $mGlu_2$ NAM analogues **13**.

Gratifyingly, this strategy afforded potent $mGlu_2$ NAMs **13a−d** (Table 1), with high selectivity versus $mGlu_3$ (IC_{50}s > 30 μM). Whereas **1** and **2** possessed cLogPs in the 3.1 to 3.6 range, analogues **13** proved less lipophilic (cLogPs 2.1 to 2.7). Across the board, analogues **13** displayed good fraction unbound in rat plasma (f_us 0.04 to 0.12) but moderate to high predicted hepatic clearance (rat CL_{hep} = 36 to 64 mL/min/kg) and high brain homogenate binding (f_u = 0.007).[26] However, the most potent analogue in this series, **13a** ($mGlu_2$ IC_{50} = 200 nM), proved to be highly CNS penetrant with a rat brain/plasma partitioning coefficient (K_p) of 2.8 and a $K_{p,uu}$ of 0.28, representing a ∼10-fold increase over historical $mGlu_2$ NAMs **1** and **2** (K_ps ≈ 0.2). Despite this exciting advance, we wished to further simplify the chemotype, reduce the number of synthetic steps, and further improve $K_{p,uu}$ and disposition.

Next, we sought to evaluate if the ethylenedioxy linker of **13** could be contracted to a simple benzyloxy linker. If tolerated, this modification would expedite the synthesis of putative $mGlu_2$ NAMs, while providing a more diverse array of functionality to modulate disposition. The synthesis of analogues **15** began with advanced intermediate **10** (Scheme 2). An S_NAr reaction sequence with diversely functionalized benzyl and heteroaryl methyl alcohols delivered **14**. In some cases, due to the presence of adventitious water, **15** was also produced in small amounts. Hydrolysis of nitrile **14** smoothly provided the desired analogues **15** in good overall yield.

DOI: 10.1021/acsmedchemlett.7b00279
ACS Med. Chem. Lett. 2017, 8, 919−924

Table 1. Structures and Activities of Analogues 13[a]

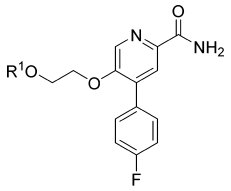

13

Entry	R^1	$mGlu_2$ IC_{50} (μM)[a] [Glu Min ±SEM]	$mGlu_2$ pIC_{50} (±SEM)	$mGlu_3$ IC_{50} (μM)[a] (pIC_{50}±SEM)
13a		0.20 [1.93±0.19]	6.70±0.08	>30 (<4.5)
13b		0.49 [2.39±0.40]	6.31±0.09	>30 (<4.5)
13c	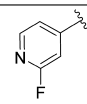	0.79 [2.39±0.46]	6.10±0.09	>30 (<4.5)
13d		0.57 [2.83±0.64]	6.24±0.09	>30 (<4.5)

[a]Calcium mobilization assays with $rmGlu_2$/TREx/Ga15-HEKcells or $rmGlu_3$/TREx/Ga15-HEK cells performed in the presence of an EC_{80} fixed concentration of glutamate; values represent means from three (n = 3) independent experiments performed in triplicate.

Scheme 2. Synthesis of Analogues 15[a]

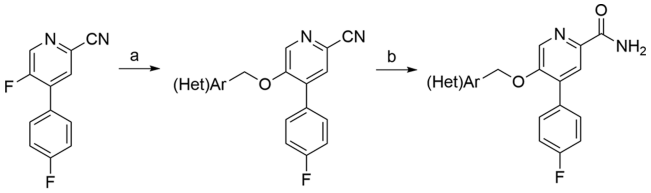

10 14 15

[a]Reagents and conditions: (a) (Het)$ArCH_2OH$, NaH, DMF, rt, 48−99%; (b) $KOSiMe_3$, THF, reflux, 80−90%.

As shown in Table 2, all analogues **15** were potent $mGlu_2$ NAMs (IC_{50}s = 78 to 560 nM) with no activity at $mGlu_3$ (IC_{50}s > 30 μM), demonstrating significant tolerability for diverse substituents. Calculated physiochemical properties were also highly favorable (cLogPs 1.9 to 3.1, TPSAs 75−90 $Å^2$, and molecular weights averaging 372). These analogues **15** displayed good fraction unbound in rat plasma (f_us = 0.04 to 0.20), but moderate to high predicted hepatic clearance (rat CL_{hep} = 48 to 65 mL/min/kg) and good brain homogenate binding (f_u = 0.046 to 0.72).[26] Of these, **15m** (VU6001966) emerged as an $mGlu_2$ NAM ($mGlu_2$ IC_{50} = 78 nM, pIC_{50} = 7.11 ± 0.10 and 1.90 ± 0.39 Glu min) without activity at $mGlu_3$ (IC_{50} > 30 μM) worthy of further evaluation. Thus, when evaluated against the full mGlu receptor family, **15m** was completely selective versus $mGlu_{1,3,4,5,6,7,8}$ in our standard 10 μM fold-shift assay.[26] We also explored broader ancillary

Table 2. Structures and Activities of Analogues 15[a]

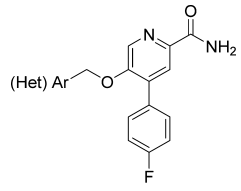

15

Entry	Ar (Het)	$mGlu_2$ IC_{50} (μM)[a] [Glu Min ±SEM]	$mGlu_2$ pIC_{50} (±SEM)	$mGlu_3$ IC_{50} (μM)[a] (pIC_{50}±SEM)
15a		0.19 [2.23±0.62]	6.71±0.07	>30 (<4.5)
15b		0.56 [5.93±1.0]	6.25±0.08	>30 (<4.5)
15c		0.21 [2.58±0.42]	6.67±0.05	>30 (<4.5)
15d	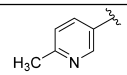	0.39 [2.77±0.44]	6.41±0.07	>30 (<4.5)
15e	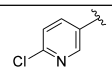	0.45 [2.14±0.26]	6.35±0.06	>30 (<4.5)
15f	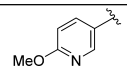	0.29 [2.21±0.37]	6.54±0.06	>30 (<4.5)
15g	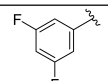	0.34 [2.94±6.54]	6.47±0.04	>30 (<4.5)
15h	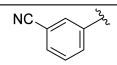	0.34 [2.34±0.37]	6.47±0.08	>30 (<4.5)
15i		0.11 [1.68±0.37]	6.96±0.06	>30 (<4.5)
15j	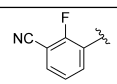	0.26 [2.54±0.63]	6.58±0.06	>30 (<4.5)
15k	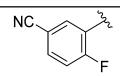	0.29 [2.20±0.26]	6.53±0.07	>30 (<4.5)
15l		0.32 [2.28±0.26]	6.49±0.12	>30 (<4.5)
15m	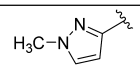	0.078 [1.90±0.39]	7.11±0.10	>30 (<4.5)

[a]Calcium mobilization assays with $rmGlu_2$/TREx/Ga15-HEKcells or $rmGlu_3$/TREx/Ga15-HEK cells performed in the presence of an EC_{80} fixed concentration of glutamate; values represent means from three (n = 3) independent experiments performed in triplicate.

DOI: 10.1021/acsmedchemlett.7b00279
ACS Med. Chem. Lett. 2017, 8, 919−924

pharmacology beyond the mGlus in a Eurofins radioligand binding panel of 68 GPCRs, ion channels, transporters, and nuclear hormone receptors and found no significant activities (no inhibition >50% @ 10 μM).[26,27] Calculated physiochemical properties were also highly favorable (cLogP 1.92, TPSAs 83 Å^2, and molecular weight of 326). These properties translated into a soluble compound (kinetic solubility of 14.7 ± 1.1 μM in PBS buffer at pH 7.4, 24 h time point) and favorable disposition. NAM **15m** displayed high fraction unbound in plasma (rat f_u = 0.20; human f_u = 0.11) and brain (rat brain f_u = 0.07), but moderate to high predicted hepatic clearance (rat CL_{hep} = 60 mL/min/kg and human CL_{hep} = 16.8 mL/min/kg) with an acceptable CYP_{450} profile (3A4, 2D6, and 2C9 IC_{50}s > 30 μM, 1A2 IC_{50} = 3.1 μM).[26] In our standard rat plasma/brain level (PBL) cassette study, **15m** demonstrated a rat K_p of 1.9, with a $K_{p,uu}$ of 0.78, values much improved over **1** and **2**, and an improved $K_{p,uu}$ over **13a**.[26] A robust *in vitro*/*in vivo* correlation (IVIVC) was noted, with a rat *in vivo* PK study showing high clearance (CL_p = 118 mL/min/kg), a short half-life ($t_{1/2}$ = 20 min), and a good volume (V_{ss} = 2.6 L/kg). Similarly, **15m** showed favorable CNS penetration in mouse as well (K_p = 0.65, $K_{p,uu}$ = 0.29), and similar PK (CL_p = 136 mL/min/kg, $t_{1/2}$ = 34 min, and V_{ss} = 5.2 L/kg). However, while [^{11}C]QCA, **2**, was limited to autoradiography due to the low CNS penetration and rodent P-gp liabilities, **15m** possesses an ideal profile for a PET tracer—high CNS penetration coupled with rapid clearance from plasma (following an IV route of administration) and desired physiochemical properties.

As this series began to position toward a candidate for PET tracer development rather than for robust *in vivo* tools suitable for proof-of-concept studies, we next evaluated the preferred aryl moiety of **2** (2-fluoro-4-methoxy phenyl) in the context of the simplified picolinamide scaffold and generated analogues **16** (Table 3) following a subtle variation of the route depicted in Scheme 2. Analogues **16** afforded the most potent $mGlu_2$ NAMs to date within this series. For example, **16c** was a potent $mGlu_2$ NAM ($mGlu_2$ IC_{50} = 26 nM, pIC_{50} = 7.57 ± 0.07, 1.81 ± 0.35 Glu min) as was **16b** ($mGlu_2$ IC_{50} = 54 nM, pIC_{50} = 7.27 ± 0.09, 2.17 ± 0.39 Glu min), and both were without activity at $mGlu_3$ (IC_{50} > 30 μM). In addition, both showed high fraction unbound in plasma (**16b**, rat f_u = 0.08, human f_u = 0.10; **16c**, rat f_u = 0.06, human f_u = 0.06), but, as with **15m**, moderate to high predicted hepatic clearance (**16b**, rat CL_{hep} = 61 mL/min/kg and human CL_{hep} = 16.0 mL/min/kg; **16c**, rat CL_{hep} = 67 mL/min/kg and human CL_{hep} = 15.8 mL/min/kg). Finally, both demonstrated high CNS penetration (K_ps of 0.34 and 1.38 and $K_{p,uu}$s of 0.15 and 0.45 for **16b** and **16c**, respectively; therefore, like **15m**, both represent attractive leads as *in vivo* PET tracers for $mGlu_2$ and overcome CNS penetration issues associated with **2**.

Before leaving **15m**, we elected to assess a dose-range mouse PBL study via intraperitoneal (IP) dosing to determine if more meaningful exposure could be achieved by bypassing first-pass metabolism. Thus, **15m** was dosed IP in male CD-1 mice at 3, 10, and 30 mg/kg (in 10% Tween80/H_2O vehicle), and plasma and brain levels were determined at a 25 min time point. As shown in Figure 3, excellent **15m** exposure was achieved in both plasma and brain across this dose-range with consistent K_ps (K_p = 1.05 @ 3 mg/kg; K_p = 1.2 @ 10 mg/kg; K_p = 1.3 @ 30 mg/kg). Total brain concentrations at the highest dose in this study were 14 μM (@30 mg/kg IP), which corresponds to ~180-fold above the $mGlu_2$ IC_{50} of **15m**, and 1.1 μM free brain (~14-fold above the $mGlu_2$ IC_{50} of **15m**). Even at 10 mg/kg IP, free brain levels were 3-fold above the $mGlu_2$ IC_{50} of **15m**. Thus, **15m** could serve as an excellent tracer candidate with IV dosing and as an *in vivo* proof of concept for $mGlu_2$ NAM via IP dosing.

Table 3. Structures and Activities of Analogues 16[a]

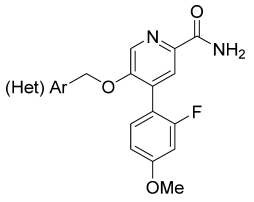

16

Entry	Ar (Het)	$mGlu_2$ IC_{50} (μM)[a] [Glu Min ±SEM]	$mGlu_2$ pIC_{50} (±SEM)	$mGlu_3$ IC_{50} (μM)[a] (pIC_{50}±SEM)
16a	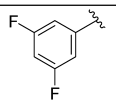	0.36 [2.44±0.43]	6.45±0.07	>30 (<4.5)
16b		0.05 [2.17±0.39]	7.27±0.09	>30 (<4.5)
16c	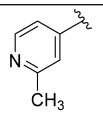	0.03 [1.81±0.35]	7.57±0.07	>30 (<4.5)
16d	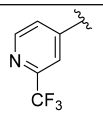	0.63 [2.43±0.55]	6.20±0.08	>30 (<4.5)
16e	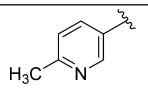	0.18 [1.94±0.39]	6.24±0.04	>30 (<4.5)
16f	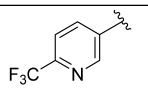	0.36 [1.78±0.56]	6.45±0.08	>30 (<4.5)

[a]Calcium mobilization assays with $rmGlu_2$/TREx/Ga15-HEKcells or $rmGlu_3$/TREx/Ga15-HEK cells performed in the presence of an EC_{80} fixed concentration of glutamate; values represent means from three (n = 3) independent experiments performed in triplicate.

In summary, we have developed the next generation of highly selective $mGlu_2$ NAMs by a reductionist strategy that also provided the first highly CNS penetrant $mGlu_2$ NAMs in both mice and rats. Excitingly, these new $mGlu_2$ NAMs possess profiles that render them attractive leads for $mGlu_2$ PET tracer development via IV dosing paradigms and have utility as *in vivo* proof of concept compounds via IP dosing. Further refinements and progress toward $mGlu_2$ NAM *in vivo* tool compounds and PET tracers are underway, and results will be reported in due course.

DOI: 10.1021/acsmedchemlett.7b00279
ACS Med. Chem. Lett. 2017, 8, 919−924

A

Dose (mg/kg)	Plasma total (μM)	Plasma free (μM)	Brain total (μM)	Brain free (μM)	K_p
3	0.23	0.04	0.28	0.02	1.05
10	2.42	0.43	2.98	0.24	1.21
30	9.94	1.75	14.0	1.12	1.37

B

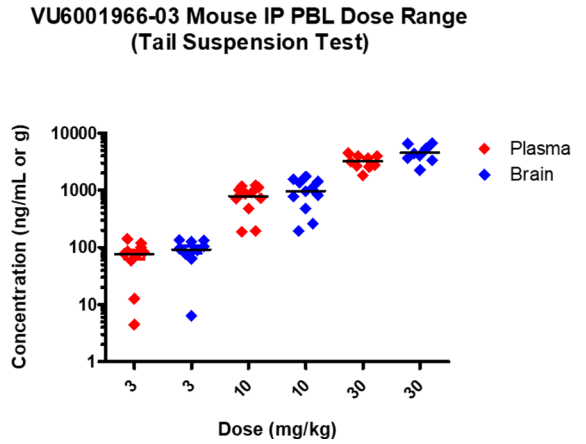

Figure 3. Exposures of **15m** (VU6001966) in plasma and brain from an IP PBL dose range study in male CD-1 mice. (A) Free and total plasma and brain concentrations achieved (3, 10, and 30 mg/kg IP). (B) Plot of plasma and brain levels achieved in the three dose groups (8–10 mice/per group).

■ ASSOCIATED CONTENT

Supporting Information

The Supporting Information is available free of charge on the ACS Publications website at DOI: 10.1021/acsmedchemlett.7b00279.

General methods for the synthesis and characterization of all compounds, methods for the *in vitro* and *in vivo* DMPK protocols, and supplemental figures (PDF)

■ AUTHOR INFORMATION

Corresponding Author

*(C.W.L) Phone: 1 615-322-8700. Fax: 1 615-936-4381. E-mail: craig.lindsley@vanderbilt.edu.

ORCID

Kyle A. Emmitte: 0000-0002-6643-3947

Craig W. Lindsley: 0000-0003-0168-1445

Present Address

⊥Department of Pharmaceutical Sciences, UNT System College of Pharmacy, University of North Texas Health Science Center, 3500 Camp Bowie Boulevard, Fort Worth, Texas 76107, United States.

Author Contributions

C.W.L. wrote the manuscript and oversaw the medicinal chemistry. K.A.E. designed compounds, and J.L.E., K.A.B., A.S.F., and C.J.B. performed chemical synthesis. P.J.C., A.L.R., H.P.C., and C.M.N. performed and analyzed molecular pharmacology data. R.L.W. performed molecular pharmacology assays. S.C. and A.L.B. oversaw and analyzed *in vitro* and *in vivo* DMPK data. C.K.J. and M.B. performed and analyzed the mouse tail suspension assay/data. All authors have given approval to the final version of the manuscript.

Notes

The authors declare no competing financial interest.

■ ACKNOWLEDGMENTS

The authors would also like to thank William K. Warren, Jr. and the William K. Warren Foundation who funded the William K. Warren, Jr. Chair in Medicine (to C.W.L.), and the National Institute of Mental Health for funding R01MH099269 (to K.A.E.).

■ ABBREVIATIONS

mGlu, metabotropic glutamate receptor; PAM, positive allosteric modulator; NAM, negative allosteric modulator; $mGlu_2$, metabotropic glutamate receptor subtype 2; PBL, plasma/brain level; K_p, plamsa/brain partitioning coefficient; $K_{p,uu}$, unbound plasma/unbound brain partitioning coefficient; IP, intraperitoneal

■ REFERENCES

(1) Niswender, C. M.; Conn, P. J. Metabotropic glutamate receptors: physiology, pharmacology, and disease. *Annu. Rev. Pharmacol. Toxicol.* **2010**, *50*, 295–322.

(2) Testa, C. M.; Friberg, I. K.; Weiss, S. W.; Standaert, D. G. Immunohistochemical localization of metabotropic glutamate receptors mGluR1a and mGluR2/3 in the rat basal ganglia. *J. Comp. Neurol.* **1998**, *390*, 5–19.

(3) Schoepp, D. D. Unveiling the functions of presynaptic metabotropic glutamate receptors in the central nervous system. *J. Pharmacol. Exp. Ther.* **2001**, *299*, 12–20.

(4) Ohishi, H.; Shigemoto, R.; Nakanishi, S.; Mizuno, N. Distribution of the messenger RNA for a metabotropic glutamate receptor, mGluR2, in the central nervous system of the rat. *Neuroscience* **1993**, *53*, 1009–1018.

(5) Ohishi, H.; Ogawa-Meguro, R.; Shigemoto, R.; Kaneko, T.; Nakanishi, S.; Mizuno, N. Immunohistochemical localization of metabotropic glutamate receptors, mGluR2 and mGluR3, in rat cerebellar cortex. *Neuron* **1994**, *13*, 55–66.

(6) Ohishi, H.; Neki, A.; Mizuno, N. Distribution of a metabotropic glutamate receptor, mGluR2, in the central nervous system of the rat and mouse: an immunohistochemical study with a monoclonal antibody. *Neurosci. Res.* **1998**, *30*, 65–82.

(7) Richards, G.; Messer, J.; Malherbe, P.; Pink, R.; Brockhaus, M.; Stadler, H.; Wichmann, J.; Schaffhauser, H.; Mutel, V. Distribution and abundance of metabotropic glutamate receptor subtype 2 in rat brain revealed by [^{3}H]LY354740 binding in vitro and quantitative radioautography: Correlation with the sites of synthesis, expression, and agonist stimulation of [^{35}S]GTPγs binding. *J. Comp. Neurol.* **2005**, *487*, 15–27.

(8) Wright, R. A.; Johnson, B. G.; Zhang, C.; Salhoff, C.; Kingston, A. E.; Calligaro, D. O.; Monn, J. A.; Schoepp, D. D.; Marek, G. J. CNS distribution of metabotropic glutamate 2 and 3 receptors: transgenic mice and [^{3}H]LY459477 autoradiography. *Neuropharmacology* **2013**, *66*, 89–98.

(9) O'Brien, N. L.; et al. The functional GRM3 Kozak sequence variant rs148754219 affects the risk of schizophrenia and alcohol dependence as well as bipolar disorder. *Psychiatr. Genet.* **2014**, *24*, 277–278.

(10) Kalinichev, M.; Campo, B.; Lambeng, N.; Célanire, S.; Schneider, M.; Bessif, A.; Royer-Urios, I.; Parron, D.; Legrand, C.; Mahious, N.; Girard, F.; Le Poul, E. An mGluR2/3 negative allo-Steric modulator improves recognition memory assessed by natural forgetting in the novel object recognition test in rats. In *Memory Consolidation and Reconsolidation: Molecular Mechanisms II; Proceedings of the 40th Annual Meeting of the Society for Neuroscience, San Diego, CA,*

Nov 13−17, 2010; Society for Neuroscience: Washington, DC, 2010; 406.9/MMM57.
(11) Choi, C. H.; Schoenfeld, B. P.; Bell, A. J.; Hinchey, P.; Kollaros, M.; Gertner, M. J.; Woo, N. H.; Tranfaglia, M. R.; Bear, M. F.; Zu-kin, R. S.; McDonald, T. V.; Jongens, T. A.; McBride, S. M. Pharmacological reversal of synaptic plasticity deficits in the mouse model of fragile X syndrome by group II mGluR antagonist or lith-ium treatment. *Brain Res.* **2011**, *1380*, 106−119.
(12) Gatti McArthur, S.; Saxe, M.; Wichmann, J.; Woltering, T. mGlu2/3 antagonists for the treatment of autistic disorders. PCT Int. Pat. Appl. WO 2014/064028 A1, May 1, 2014.
(13) Structure of decoglurant disclosed in Recommended International Nonproprietary Names (INN). In *WHO Drug Information*; World Health Organization: Geneva, Switzerland, 2013; Vol. *27*, no. 3, p 150.
(14) ARTDeCo Study: A study of RO4995819 in patients with major depressive disorder and inadequate response to ongoing antidepressant treatment. ClinicalTrials.gov; U.S. National Institutes of Health: Bethesda, MD, 2011; https://www.clinicaltrials.gov/ct2/show/NCT01457677.
(15) Lindsley, C. W.; Emmitte, K. A.; Hopkins, C. R.; Bridges, T. M.; Gregory, K. J.; Niswender, C. M.; Conn, P. J. Practical Strategies and Concepts in GPCR Allosteric Modulator Discovery: Recent Advances with Metabotropic Glutamate Receptors. *Chem. Rev.* **2016**, *116*, 6707−6741.
(16) Trabanco, A. A.; Cid, J. M. mGluR2 positive allosteric modulators: a patent review (2009-present). *Expert Opin. Ther. Pat.* **2013**, *23*, 629−647.
(17) Sheffler, D. J.; Wenthur, C. J.; Bruner, J. A.; Carrington, S. J. S.; Vinson, P. N.; Gogi, K. K.; Blobaum, A. L.; Morrison, R. D.; Vamos, M.; Cosford, N. D. P.; Stauffer, S. R.; Daniels, J. S.; Niswender, C. M.; Conn, P. J.; Lindsley, C. W. Development of a novel, CNS-penetrant, metabotropic glutamate receptor 3 (mGlu3) NAM probe (ML289) derived from a closely related mGlu5 PAM. *Bioorg. Med. Chem. Lett.* **2012**, *22*, 3921−3925.
(18) Wenthur, C. J.; Morrison, R.; Felts, A. S.; Smith, K. A.; Engers, J. L.; Byers, F. W.; Daniels, J. S.; Emmitte, K. A.; Conn, P. J.; Lindsley, C. W. Discovery of (R)−(2-fluoro-4-((−4-methoxy phenyl)ethynyl)-phenyl(3-hydroxypiperidin-1-yl)methanone (ML337), an mGlu3 selective and CNS penetrant negative allosteric modulator (NAM). *J. Med. Chem.* **2013**, *56*, 5208−5212.
(19) Walker, A. G.; Wenthur, C. J.; Xiang, Z.; Rook, J. M.; Emmitte, K. A.; Niswender, C. M.; Lindsley, C. W.; Conn, P. J. Metabotropic glutamate receptor 3 activation is required for long-term de-pression in medial prefrontal cortex and fear extinction. *Proc. Natl. Acad. Sci. U. S. A.* **2015**, *112*, 1196−1201.
(20) Engers, J. L.; Rodriguez, A. L.; Konkol, L. C.; Morrison, R. D.; Thompson, A. D.; Byers, F. W.; Blobaum, A. L.; Chang, S.; Loch, M. T.; Niswender, C. M.; Daniels, J. S.; Jones, C. K.; Conn, P. J.; Lindsley, C. W.; Emmitte, K. A. Discovery of VU0650786: A selective and CNS penetrant negative allosteric modulator of metabotropic glutamate receptor subtype 3 with antidepressant and anxio lytic activity in rodents. *J. Med. Chem.* **2015**, *58*, 7485−7500.
(21) Engers, J. L.; Bollinger, K. A.; Rodriguez, A. L.; Long, M. F.; Breiner, M. M.; Chang, S.; Bubser, M.; Jones, C. K.; Morrison, R. D.; Bridges, T. M.; Blobaum, A. L.; Niswender, C. M.; Conn, P. J.; Emmitte, K. A.; Lindsley, C. W.; Weiner, R. L.; Bollinger, S. R. Design and Synthesis of *N*-Aryl Phenoxyethoxy Pyridines as Highly Selective and CNS Penetrant mGlu3 NAMs. *ACS Med. Chem. Lett.* **2017**, x DOI: 10.1021/acsmedchemlett.7b00249. Companion paper.
(22) Felts, A. S.; Rodriguez, A. L.; Smith, K. A.; Engers, J. L.; Morrison, R. D.; Byers, F. W.; Blobaum, A. L.; Locuson, C. W.; Chang, S.; Venable, D. F.; Niswender, C. M.; Daniels, J. S.; Conn, P. J.; Lindsley, C. W.; Emmitte, K. A. Design of 4-Oxo-1-aryl-1,4-dihydroquinoline-3-carboxamides as selective negative allosteric modulators of metabotropic glutamate receptor subtype 2. *J. Med. Chem.* **2015**, *58*, 9027−9040.
(23) Zhang, X.; Kumata, K.; Yamasaki, T.; Cheng, R.; Hatori, A.; Ma, L.; Zhang, Y.; Xie, L.; Wang, L.; Kang, H. J.; Sheffler, D. J.; Cosford, N. D. P.; Zhnag, M.-R.; Liang, S. H. Synthesis and Preliminary Studies of a Novel Negative Allosteric Modulator, 7-((2,5- Dioxopyrrolidin-1-yl)methyl)-4-(2-fluoro-4-[^{11}C]methoxyphenyl) quinoline-2-carboxamide, for Imaging of Metabotropic Glutamate Receptor 2. *ACS Chem. Neurosci.* **2017**, DOI: 10.1021/acschemneuro.7b00098.
(24) Samadi, P.; Rajput, A.; Calon, F.; Grégoire, L.; Hornykiewicz, O.; Rajput, A. H.; Di Paolo, T. Metabotropic Glutamate Receptor II in the Brains of Parkinsonian Patients. *J. Neuropathol. Exp. Neurol.* **2009**, *68*, 374−382.
(25) Lee, H. G.; Zhu, X.; O'Neill, M. J.; Webber, K.; Casadesus, G.; Marlatt, M.; Raina, A. K.; Perry, G.; Smith, M. A. The role of metabotropic glutamate receptors in Alzheimer's disease. *Acta Neurobiol. Exp.* **2004**, *64*, 89−98.
(26) See Supporting Information for full details.
(27) LeadProfilingScreen; (catalogue no. 68) Eurofins Panlabs, Inc.: Redmond, WA (www.eurofinspanlabs.com).

NOTE ADDED AFTER ASAP PUBLICATION

This paper was published ASAP on August 18, 2017, with an error in the Supporting Information. The corrected version was reposted on August 25, 2017.

DOI: 10.1021/acsmedchemlett.7b00279
ACS Med. Chem. Lett. 2017, 8, 919−924